Proceedings of the 21st ICSMGE, Vienna, Austria, 14 – 19 June 2026. Pistrol, Adam & Schweiger (eds.)
Published by: ÖGG, Austrian Society for Geomechanics, Salzburg, Austria, ISBN 978-3-9503898-4-5
https://doi.org/10.53243/ICSMGE2026-1415

A case study of multi-storey buildings construction in urban areas over underground limestone mines

Yuriy Vynnykov, Maksym Kharchenko
National university "Yuri Kondratyuk Poltava Polytechnic", Ukraine, vynnykov@ukr.net

Vasyl Mitinsky
Odesa State Academy of Architecture and Civil Engineering, Ukraine

Valentyn Marchenko
LLC "Scientific and Technical Company "ALMAGROUP", Poltava, Ukraine

ABSTRACT: Modern residential complexes in Odesa city are built of more than 20 stories cast-frame superstructures with a common stylobate and a single or multi-level underground parking. The projects are complicated by the presence of a low-thickness limestone-shell rock layers in the massif at a depth of 26-30 m from the surface and underlain by more compressible soils. The layers contain underground mines with a cross-section of up to 2.4×5.0 m. The limestone-shell rocks have very low strength – less than 2.0 MPa. Underground mines were developed in the mid-nineteenth century. They don't have reliable supports and occupy up to 25-40% of the construction site. The geotechnical project considers: the technical state of underground mines; possible complications during pile boring above the mines; shear bearing capacity of the limestone thickness, taking into account the more compressed soils beneath them; the impact of the filled mines on the overlying massif; the deterioration of these factors under seismic impacts. The limestone parameters above the mines were tested in-situ and in laboratory. Hydraulic grouting of cavities by sand slurry and compacting of its vault with grouting solution has been tested. The experiment results on the use of soil cement as a slurry are presented. Two types of slurry have been tested for reliable fixing of sand-filled mine: with superplasticizers addition for high mobility, low water loss, non-shrinkage after hardening; with a high degree of spreading. In order to perceive tensile forces within underground mines arising from tangential stresses along the shear surfaces. The effectiveness of additional reinforcing elements from bored piles is substantiated. The experience of 3D finite element modeling of pile-slab foundation and geodetic monitoring results are presented. The geotechnical solutions of multi-storey buildings construction in urban areas over underground limestone mines are summarized.

KEYWORDS: underground mines, fissured limestone, stress-strain state, punching shear, grouting solution.

1 INTRODUCTION

Shell limestone of Pontian age was the primary construction material for the vast majority of buildings in Odesa until the early 20th century. The material was extracted directly from beneath the current city site. As a result, numerous underground limestone mines, locally known as "catacombs", were formed. In some cases, these are small horizontal cavities extending for only tens of meters; in others, they form vast labyrinthine systems stretching for tens of kilometers, sometimes arranged in two tiers. The length of underground quarries only in the modern city boundaries is about 600 km.

The ongoing urban development necessitates the use of areas that were previously considered only marginally suitable for construction. The increasing height of buildings results in greater loading on foundations. At the same time, construction is carried out in confined urban settings and on sites with complex geotechnical conditions, including subsurface mines.

Due to numerous influencing factors such as formation conditions, weathering processes, and anthropogenic activity, the geotechnical properties of limestones exhibit significant spatial heterogeneity and considerable variation in strength parameters (Aladejare 2017). As a result, regional approaches to laboratory and in-situ evaluation of different limestone varieties have become widespread. These assessments account for the predominant orientation of fissures or localized zones of weakness (Wong 2015), the presence of normal faults (Gemayel 2020), and the degree of pore water saturation (Dweirj 2017), enabling the derivation of empirical correlations between physical and mechanical properties.

Three-dimensional finite element modeling has been applied to assess the stability of both natural and anthropogenic underground cavities, as well as to evaluate the development of weakened (fissured) zones within limestone massifs (Castellanza 2013). This approach is typically combined with geodetic and geophysical monitoring methods (Zenah 2020). The most reliable results are achieved when the models incorporate the strength anisotropy of fissured rock masses and established geotechnical failure criteria (Barton 2007). The Mohr-Coulomb criterion is commonly used to evaluate the failure of intact rock and discrete joints (Chang 2018), whereas the Hoek-Brown criterion provides a reasonably accurate estimation of rock mass strength based on the properties of intact rock and the degree of jointing (Prountzopoulos 2011).

For high-rise buildings founded on limestone massifs, including those with underlying cavities, piled-raft foundations have demonstrated high reliability Both driven steel piles (McCullough 2013) and bored cast-in-place piles (Alshenawy 2018) have proven effective. In conditions of dense urban development, ground improvement using soil-cement elements installed via deep mixing (Kryvosheiev 2017) or jet grouting (Ovando-Shelley 2022) has also shown positive results.

Thus, the development of reliable foundations for limestone massifs containing underground mines requires experimental justification, a consistent modeling approach, and special methods for construction monitoring. This constitutes an important challenge in geotechnical engineering. Further research is needed to investigate the influence of discrete weakened zones on the stress–strain state of the foundation under additional loading, to assess the potential shear failure surfaces in limestones, and to improve current design methods.

2 SPECIFIC FEATURES OF UNDERGROUND LIMESTONE MINES IN ODESA

The thickness of the Pontic limestone can be divided into 4 layers. Layer 1 (the deepest) consists of platy limestone with a thickness ranging from 0.2 to 1.0 m. Layer 2 is a uniformly cemented limestone-shell rock (commonly referred to as "sawn" limestone) with a thickness of 4.5 to 7.9 m. The underground mines are located within this layer. Their dimensions and density depend on the quality of the limestone (Figure 1). Layer 3 comprises highly recrystallized limestone-shell rock. Layer 4, the uppermost, is a platy-detrital limestone with clayey infill. The combined thickness of Layers 3 and 4 is approximately 5.0 to 5.6 m. The entire limestone massif is overlain by dense clays.

The limestone extraction site represents a large mining field composed of interconnected small-scale mines (Figure 1a) that have undergone collapses, debris clearance, initial support installation, new crosscuts, repeated strengthening over time. Some of these mines have been backfilled, others are reinforced with concrete walls, while the rest remain unsupported.

Test boreholes were drilled to identify the location of inaccessible workings where backfilling had previously been carried out, including the method and quality of the backfill. It was determined that in areas where water-sand slurry was used for backfilling, cavities ranging from 0.2 to 0.8 m remained between the mine top (roof) and the sand fill.

When drill tool failure (sudden drop) was observed during borehole advancement, a borehole camera was lowered to inspect and record the void geometry. In the area of a local mine, a shaft with a diameter of 630–720 mm was drilled, allowing for direct inspection of the cavity (Figure 1b).

a

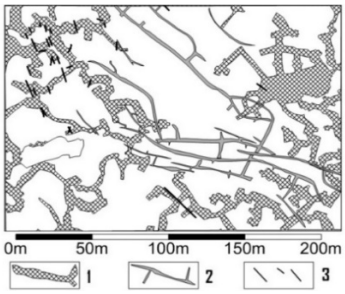

b

Figure 1. Fragment of the subsurface void area (a) and cross-section of the mines (b): 1 - underground mines ("catacombs"); 2 - karst cavities; 3 - fissures affected by karstification.

3 SOIL LOOSENING ABOVE THE MINES

Previously, after stone extraction was completed, the resulting cavities in the mines were not backfilled. It was considered sufficient to stabilize them by constructing rudimentary supports made of substandard stone blocks, especially in the then-unsaturated host rock. Over time, however, the influence of both natural factors (such as changes in hydrogeological conditions and in-situ stresses) and anthropogenic activities (such as the drilling of drainage, exploratory, and technological boreholes, as well as urban development) led to collapses caused by roof failures of unsupported workings.

This degradation process was intensified by rising groundwater levels. According to borehole data and cone penetration testing (Figure 2), zones of soil loosening have been identified above some of the mines. A weakened zone has formed up to 10-12 m thickness consisting of collapsed roof material (Figure 3), the void and the loosened soil overlying it.

The mine voids were typically filled by injecting a water-sand slurry into the cavities. Following this, the surrounding rock mass was strengthened by high-pressure grouting with cement or soil-cement mixtures.

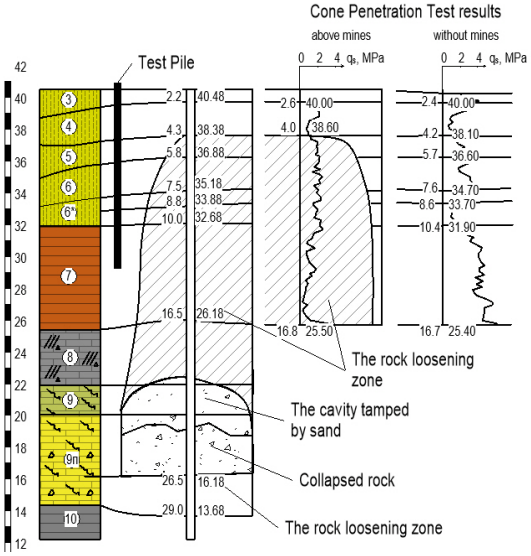

Figure 2. Collapse zones of mine roofs and soil loosening: 3-6 – loess-like loams; 7 – clay; 8 – limestone rubble and slabs with clayey infill;
9 – platy, recrystallized limestone; 9п – "sawn" limestone; 10 – clay.

Figure 3. Fragment of a mine cavity affected by roof collapse.

To verify the quality of soil cementation, control boreholes were drilled, and soil samples were collected from them (Figure 4). For each specimen, the bulk density and dry density were determined (Table 1). Corresponding values obtained prior to cementation are also provided for comparison. Static load tests on piles were conducted both before and after cementation. As a result of cementation, the bearing capacity of the soil increased by 35%.

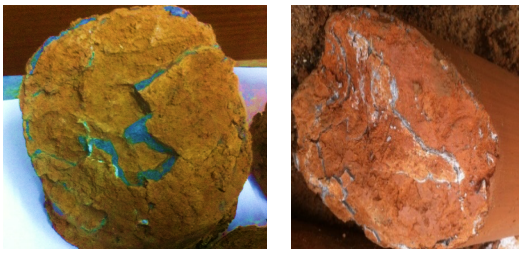

Figure 4. Samples from the strengthened soil mass above mine workings with collapsed roofs.

Table 1. Data on bulk and dry density of the soil.

	Symbol	Value before improvement	Value after improvement	Unit
Soil layer 6				
Bulk density	ρ	1.89…1.90	1.92…1.98	g/cm^3
Dry density	ρ_d	1.54…1.55	1.55…1.64	g/cm^3
Soil layer 7				
Bulk density	ρ	1.85…1.86	1.90…1.97	g/cm^3
Dry density	ρ_d	1.44…1.45	1.51…1.60	g/cm^3
Soil layer 7з				
Bulk density	ρ	1.81…1.85	1.87…1.90	g/cm^3
Dry density	ρ_d	1.45…1.46	1.53…1.54	g/cm^3
Soil layer 7к				
Bulk density	ρ	1.74…1.75	1.79…1.85	g/cm^3
Dry density	ρ_d	1.30…1.31	1.38…1.41	g/cm^3

4 INVESTIGATION OF MECHANICAL PROPERTIES OF LIMESTONES

Young's modulus, Poisson's ratio, shear and compressive strength of limestones were studied in field and laboratory conditions. The deformation modulus at various depths within the limestone sequence was determined by plate loading tests in the boreholes using a 45 cm diameter plate. After reaching the in-situ stress level, the load was increased in increments of 0.1 MPa (Table 2).

Table 2. Young's modulus values of limestones from plate load tests at various depths.

	Symbol	Value	Unit
Soil layer 9 (depth 19 m)			
Poisson's ratio	ν	0.38	-
Young's modulus	E	85	MPa
Soil layer 10 (depth 21 m)			
Poisson's ratio	ν	0.20	-
Young's modulus	E	123	MPa
Soil layer 11 (depth 27 m)			
Poisson's ratio	ν	0.20	-
Young's modulus	E	50	MPa
Soil layer 12 (depth 30 m)			
Poisson's ratio	ν	0.20	-
Young's modulus	E	111	MPa

The anisotropy parameters of the shell limestone were determined using a modified oedometer. Samples extracted at different angles to the vertical were fixed in a steel ring with a diameter of 86 mm. The loading plate had a diameter of 43.7 mm (an area of 15 cm²), simulating soil behavior within the rock mass with allowance for lateral deformations. The results of the anisotropy study are presented in Figure 5.

To refine the design shear strength of sawn shell limestone, a series of samples were tested in direct shear. The test was carried out along two vertical shear planes oriented parallel to the applied load with a total shear plane area of 200 cm². The average shear strength was 0.48 MPa, with a standard deviation of 0.29 MPa. The shear resistance, defined as the minimum shear strength value at a 75% confidence level, was determined to be 0.22 MPa. Punching tests on the samples (Figure 6) yielded values similar to the shear strength.

To determine the Poisson's ratio, cubic limestone specimens (200×200×200 mm) were tested in uniaxial compression. Steel rods with a diameter of 4 mm were rigidly embedded in each cube in orthogonal directions (Figure 7), and the changes in distance between the rods were measured during loading. The test results showed an average unconfined compressive strength of 0.73 MPa with a standard deviation of 0.12 MPa. The design compressive strength, defined as the lowest strength value at a 75% confidence level, was 0.57 MPa. The measured Poisson's ratio was 0.2.

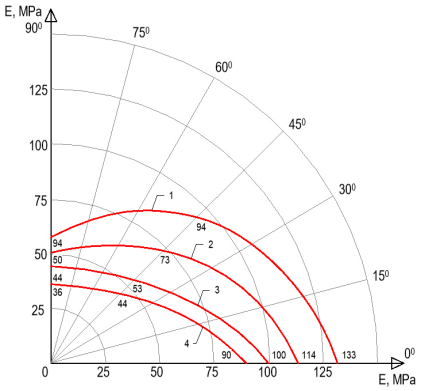

Figure 5. Polar plots of the dependence of deformation modulus on loading direction within the following pressure intervals: 1-0-0.25 MPa; 2 – 0.25-0.5 MPa; 3 – 0.5-0.75 MPa; 4 – 0.75-1.0 MPa

Figure 6. Punching test of limestone samples

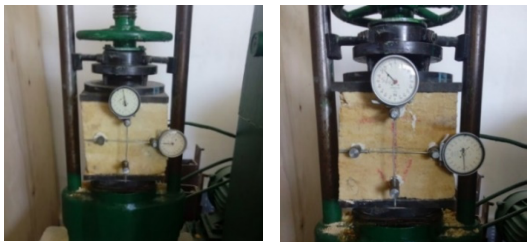

Figure 7. Uniaxial compression test of limestone specimens

5 STRUCTURAL AND TECHNOLOGICAL SOLUTIONS FOR STABILIZING SOIL MASSIF

At the construction site of a 24-storey residential building underground mines were identified at a depth of approximately 30 m below ground level. They occupied more than 26% of the building footprint (Figure 8a) and had previously been backfilled with a water-sand slurry. However, it was found that the voids were not completely filled with sand throughout their height. Under additional loading, their stability could not be guaranteed, and additional strengthening was deemed necessary. Due to the limited height of the cavities (0.4-0.8 m), access was restricted. Therefore, a set of reliable reinforcement solutions was developed. The first stage involved the elimination of the cavities, while the second focused on consolidation of the backfill material and strengthening of the rock mass above the excavations (Figure 8b). The ultimate objective of these measures was to create a quasi-homogeneous compressible layer within the foundation zone affected by the presence of underground voids.

At the first stage, the interconnected cavities – communicating with each other and with previously drilled boreholes – were filled. Two types of cement-sand grouts were used for this purpose: (1) mixes with superplasticizers to

ensure high flowability, low water separation, and no shrinkage after hardening; (2) mixes without superplasticizers but with a high degree of spreadability. The grout was delivered either by gravity feed into the borehole or by pump under pressures up to 1 MPa. The degree of cavity filling was monitored using a "flapper" tool, which was lowered into both working and control boreholes.

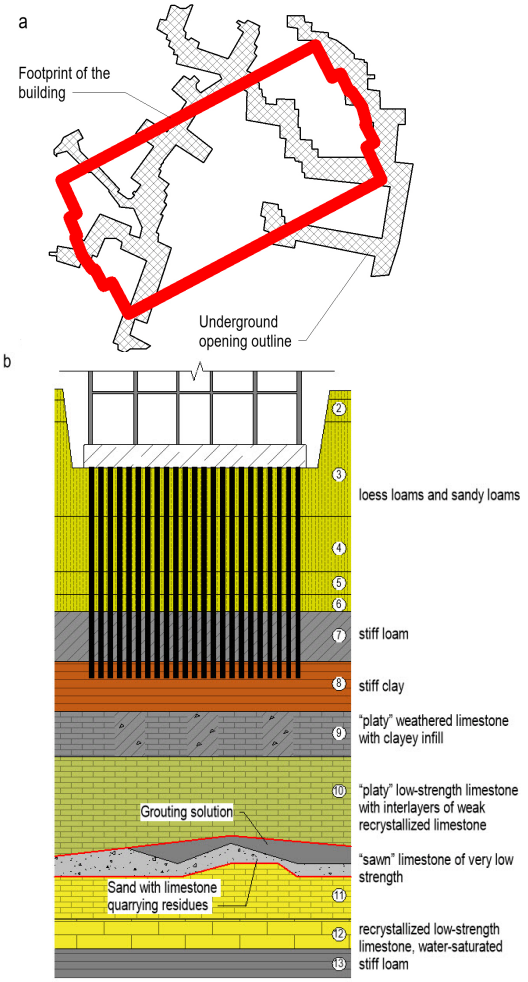

Figure 8. Location of mines in top view (a) and cross-section (b).

At the second stage, grout was injected through sleeve port pipes into the excavations and into the rock mass located up to 3 m above the roof of the catacombs. In top view, the sleeve pipes were positioned between the grout injection boreholes, and vertically they were arranged at 1 m intervals, starting from the floor of the excavation. The subsoil reinforcement in the mine area was carried out in the following sequence. A sleeve port pipe with a diameter of 86 mm was installed into the injection borehole with a diameter of 168 mm. The annular space between the pipe and the borehole wall was filled with low-strength cement grout. After 24 hours, a soil-cement grout was injected into the rock mass. It was delivered through the sleeve ports under a pressure of 3-4 MPa, proceeding sequentially from the bottom port to the top. If the injection pressure exceeded 4.5 MPa, the process was stopped.

The project (Figure 8b) uses a piled-raft foundation consisting of piles with a cross-section of 35×35 cm and a length of 14 m, with their lower ends embedded in Layer 8 – hard clay. The raft thickness is 1.8 m. Beneath the clay lies a limestone massif, within the cuttable limestone layer of which the underground mines were identified. Their influence was mitigated prior to the foundation installation.

6 SIMULATION OF LIMESTONE LAB TEST

Selecting an appropriate constitutive model for limestone behavior is complicated by the dual nature of these materials. On one hand, they are semi-rock, cemented soils that can be described as continuous rock masses; on the other hand, their significant porosity, stratification, and fracturing result in considerably lower strength and higher deformability compared to intact rock. Two main approaches exist for modeling rock masses with substantial heterogeneity due to their specific structure and fracturing.

The first approach involves explicitly defining the orientation and position of fractures, assigning different parameters to the intact rock and the fractures. Typically, fracture behavior is modeled by "smeared" representation across the mass with certain coefficients introduced. For example, the Jointed Rock Model in the Plaxis software considers only the fracture orientation angle and allows for input of parameters in the tangential (along fractures) and normal (across fractures) directions. However, this model is suitable primarily when fractures have a well-defined orientation, which is not typical for shell limestone.

The alternative approach, applicable to rock masses with chaotic fracturing, is embodied in the Hoek–Brown (HB) model. This model is more appropriate for limestones as it empirically accounts for fracture characteristics, degree of disturbance due to excavation, and the strength of intact rock.

The HB model is implemented in the Plaxis software by means of Equations (1)-(4). It incorporates generalized parameters, including the Geological Strength Index (GSI) – a coefficient determined by visual inspection of sample surfaces that accounts for fracturing and rock surface nature; m_i – an empirical parameter known as the intact rock constant, which describes the curvature of the nonlinear relationship between the major (σ_1) and minor (σ_3) principal stresses for intact rock (i. e., without fractures or defects). A higher m_i – value indicates a more brittle rock behavior under loading; and D – the disturbance factor, ranging from 0 for intact rock masses to 1 for heavily disturbed rock masses due to excavation.

$$\sigma_1 = \sigma_3 + \sigma_{ci} \cdot \left(m_b \cdot \left(\frac{\sigma^3}{\sigma_{ci}}\right) + s \right)^a, \quad (1)$$

$$m_b = m_i \cdot exp\left(\frac{GSI - 100}{28 - 14 \cdot D}\right), \quad (2)$$

$$s = exp\left(\frac{GSI - 100}{9 - 3 \cdot D}\right), \quad (3)$$

$$a = \left(\frac{1}{2}\right) + \left(\frac{1}{6}\right) \cdot \left[\exp\left(\frac{-GSI}{15}\right) - \exp\left(-\frac{20}{3}\right)\right]. \quad (4)$$

A separate issue concerns the strength of intact rock, the value of which is difficult to determine directly through sample testing due to existing defects in the rock. In such cases, inverse analysis is used, starting from the known strength of fractured samples. Given that the average strength of the tested rock is 0.73 MPa, and considering the relevant coefficients, the accepted intact rock strength is taken as 8.9 MPa.

A benchmark simulation of laboratory tests is carried out for reproducing the mechanical behavior of limestone specimens subjected to uniaxial compression and direct shear. Such numerical modeling enables the evaluation of the adequacy of the adopted model parameters.

Finite element modeling (FEM) of specimen under unconfined compression conditions was conducted corresponding to laboratory tests (Figure 7), with vertical pressure applied to the top face. The maximum load applied to the specimen corresponds to a unconfine compressive strength (UCS) of 0.73 MPa. The overall appearance of the specimen

and its deformations after compression are shown in Figure 9. Under this load, zones of plastic deformation develop within the mass (Figure 10), and the material enters the plastic deformation stage, meaning the specimen fails.

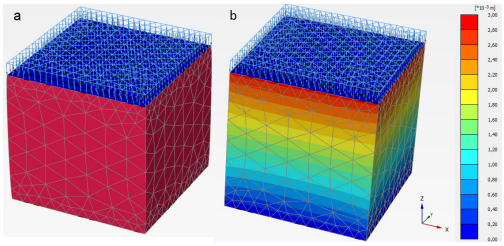

Figure 9. Modeling of compressive tests on specimens: (a) overall view of the specimen with finite element mesh; (b) contour plot of total strain in the specimen.

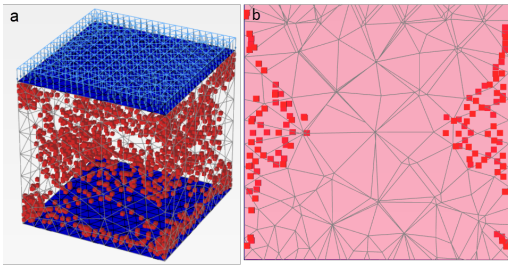

Figure 10. Plastic points within the specimen volume (a) and along the vertical cross-section of the specimen (b).

To refine the model parameters in terms of shear strength, the corresponding tests of limestone samples were simulated (Figure 11). The load applied to the midsection of the specimen corresponded to the average shear strength value of 0.48 MPa measured on two shear planes. The distribution of shear stresses and plasticity (Figure 12), was obtained, showing full agreement with laboratory test data (Figure 6). The destruction of the sample occurs with the formation of inclined zones of plasticity, which, as they increase, form a continuous zone of displacement along predetermined planes. The HB model parameters for the tested limestone are presented in Table 3.

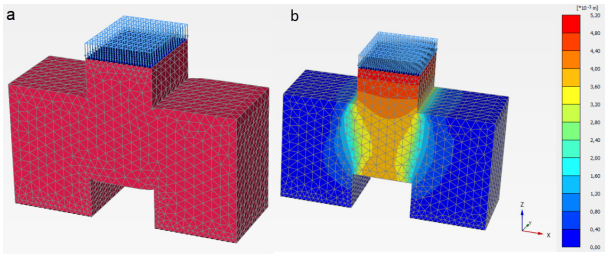

Figure 11. Modeling of shear tests on specimens: (a) overall view of the specimen with finite element mesh; (b) contour plot of total strain in the specimen.

Table 3. Hoek-Brown (HB) model parameters.

Parameter	Symbol	Value	Unit
Unit weight	γ	20	kN/m^3
Young's modulus	E	50	MPa
Poisson's ratio	ν	0.2	-
Uniaxial compression strength of intact matrix	σ_{ci}	8900	kPa
Hoek-Brown constant for intact rock	m_i	7	-
Geological Strength Index (GSI)	GSI	55	-
Disturbance factor	D	0.0	-

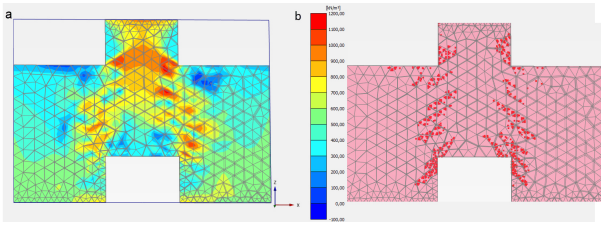

Figure 12. Modeling of shear tests on specimens: (a) overall view of the specimen with finite element mesh; (b) contour plot of total strain in the specimen.

7 MODELING OF THE INTERACTION BETWEEN FOUNDATIONS AND THEIR SOIL BASES CONTAINING DISORDERLY DISTRIBUTED EXCAVATIONS

The modeling of the interaction between foundations and their soil bases containing excavations was performed using a piled-raft foundation design scheme based on the cross-section and layout of the excavations (Figure 8). Figure 13 presents the 3D finite element modeling scheme. The simulation was conducted to predict maximum settlements and evaluate stress levels within the limestone massif, considering all structural and technological reinforcement measures for the massif weakened by excavations as described in Section. The HB model with parameters corresponding to the design properties (Section 4) was adopted to simulate the behavior of the limestones.

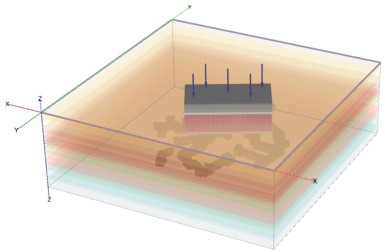

Figure 13. Finite element model for analyzing the interaction between foundations and their soil bases containing underground mines.

The stress levels in rock mass weakened by the excavations were evaluated using contour plots of the distribution of maximum shear and tangential stresses around the excavations. Figure 14 presents contour plots of shear stresses at the roof level of the excavations. It shows that the average shear stress values along the upper boundary of the excavations reach up to 200 kPa, with peak values rising to 360 kPa due to stress concentration at the sharp corners of the excavations.

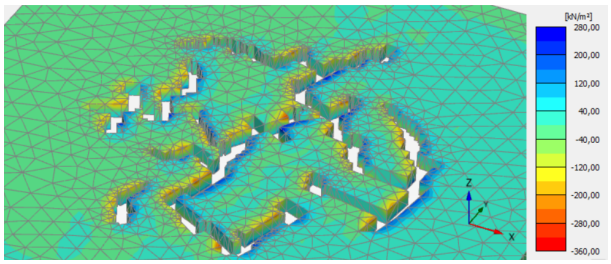

Figure 14. Contour plots of shear stresses prior to loading from the new construction.

Figure 15 presents contour plots of shear stresses at the top level of the mines after they were filled with soil-cement grout and subjected to the full building load. The plots demonstrate that the shear stresses remain essentially unchanged, confirming the soundness of the adopted excavation filling method. Modeling results indicate (Figure 16) that maximum settlements under full foundation loading will be 11.4 cm.

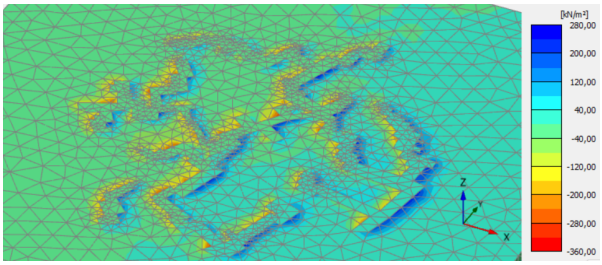

Figure 15. Contour plots of shear stresses after filling voids with soil-cement grout and applying full construction loading.

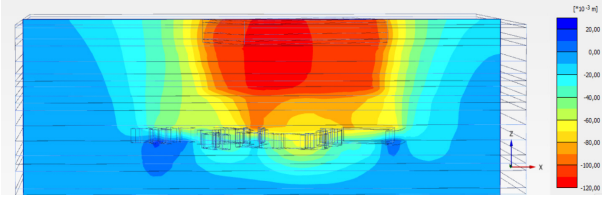
Figure 16. Contour plots of total strains along the cross-section.

8 MONITORING OF THE STRUCTURE

The composition of the soil-cement grout was controlled in the laboratory. The loam consumption was set at 1 m³ by bulk density per 1 m³ of soil-cement, while the cement dosage was adjusted stepwise from 80 to 200 kg/m³ to achieve the specified strength. According to monitoring results, the average penetration width of the grout was 2-2.5 m.

Four identical residential buildings are currently being constructed on site, with instrumental monitoring of their settlements. A comparison of settlement development curves over time, under the same load level (66% of the design load), between the test building and a similar structure founded on ground without excavations showed no significant influence of the previously weakened but subsequently reinforced zones on the foundation deformation (Table 4). This indicates the quality of the work performed to mitigate the impact of the mines on the overall behavior of the foundations and soil base. Settlements develop uniformly along the entire building perimeter.

Table 4. Settlement rate of buildings depending on the loading rate.

Building ground base	Base load, kN	Duration, day	Settlement, mm	Settlement rate, mm/day
Without mines	50400	346	33.09	0.096
With mines	50400	579	25.2	0.044

9 CONCLUSIONS

The geotechnical conditions of Odesa are characterized by interlayers of limestone in the upper part of the section. Shell limestone exhibits low compressive and shear strength, as well as disorderly distributed weakened zones, including mines, which necessitate stabilization to create a quasi-homogeneous mass within the compressed foundation soil layer.

The reliability of the limestone foundation with weakened areas is ensured by backfilling with a hydraulic sand wash followed by injection of soil-cement grout into both the backfilled zone and the overlying weakened sections.

Based on laboratory and field tests, the mechanical parameters of shell limestones were determined: at a 75% confidence level, the shear strength is 0.22 MPa, while the minimum compressive strength is 0.57 MPa. The compressibility of the limestones is characterized by varying degrees of anisotropy within each layer. The Young's moduli of the limestone layers range from 50 to 123 MPa.

The parameter values for the Hoek–Brown model were calibrated through 3D finite element modeling of the laboratory limestone tests, demonstrating that the model adequately simulates the behavior of Pontian limestones in Odesa. Modeling of the interaction between foundations and their soil bases containing chaotically distributed excavations showed that the project's design solution for filling existing voids with soil-cement grout effectively mitigates additional shear stresses in the limestone massif weakened by the mining.

Monitoring of the building construction on limestone layers containing excavation-weakened zones that were stabilized prior to construction showed that the settlements did not exceed those recorded for similar buildings founded on intact ground. Furthermore, the settlement progression was uniform along the building perimeter.

REFERENCES

Aladejare, A. E., and Wang, Y. 2017. Evaluation of rock property variability. Georisk: Assessment and Management of Risk for Engineered Systems and Geohazards, 11 (1), 22-41.

Wong, L. N. Y., Maruvanchery, V., and Oo, N. N. 2015. Engineering properties of a low-grade metamorphic limestone. Engineering Geology, 193, 348-362.

Gemail, K.S., Shebl, S., Attwa, M., Soliman, S.A., Azab, A., and Farag, M.H. 2020. Geotechnical assessment of fractured limestone bedrock using DC resistivity method: a case study at New Minia City, Egypt. NRIAG Journal of Astronomy and Geophysics, 9: 1, 272-279.

Dweirj, M., Fraige, F., Alnawafleh, H., and Titi, A. 2017. Geotechnical Characterization of Jordanian Limestone. Geomaterials, 7, 1-12.

Castellanza, R., Lollino, P., Ciantia, M. O., di Prisco, C., Crosta, G., and Frigerio, G. 2013. Numerical analysis for the evaluation of the stability of underground cavities in calcarenite interacting with buildings. Proc. European Geosciences Union General Assembly. Vienna Austria. Available at: https://www.researchgate.net/publication/258784213

Zenah, J., Görög. P., and Pasierb, B. 2020. Exploration and stability analysis of underground cavities of urban areas. Proc. 6th Intern. Conf. on Geotechnical and Geophysical Site Characterization (ISC2020). Budapest, Hungary. Available at: https://doi.org/10.53243/ISC2020-192

Barton, N. 2007. Rock Quality, Seismic Velocity, Attenuation and Anisotropy. Taylor & Francis Group, London, UK.

Chang, L., and Konietzky, H. 2018. Application of the Mohr-Coulomb Yield Criterion for Rocks with Multiple Joint Sets Using Fast Lagrangian Analysis of Continua 2D (FLAC2D) Software. Energies, 11(3), 614.

Fortsakis, P., Balasi, A.M., Prountzopoulos, G., Marinos, P., and Marinos V. 2011. Comparative study of the use of Hoek-Brown and equivalent Mohr-Coulomb parameters in tunnel excavation. In book: Géologie de l' Ingénieur. Hommage à la mémoire de Marcel Arnould. Publisher: Press de l'Ecole des Mines.

McCullough, N.J., and Dorang, C. 2013. Foundation Design in Weathered Limestone - Where Will the Piles End? Proc. 13th Intern. Conf. Ports: Success through Diversification. Available at: https://doi.org/10.1061/9780784413067.132

Alshenawy, A., Hamid, W., and Alnuaim, A. 2018. Skin friction behavior of pile fully embedded in limestone. Arabian Journal of Geosciences, 11(2).

Kryvosheiev, P., Farenyuk, G., Tytarenko, V., Boyko, I., Kornienko, M., Zotsenko, M., Vynnykov, Yu., Siedin, V., Shokarev, V., and Krysan, V. 2017. Innovative projects in difficult soil conditions using artificial foundation and base, arranged without soil excavation. Proc. 19th Intern. Conf. on Soil Mechanics and Geotechnical Engineering. Seoul. ICE Publishing, 3007-3010.

Ovando-Shelley, E, Botero-Jaramillo, E., and Díaz-Guzmán, M. A. 2022. Jet Grouting to mitigate damage induced by tunneling near the church of San Francisco de Asis in Guadalajara, Mexico Proc. 20th Intern. Conf. on Soil Mechanics and Geotechnical Engineering, 2. Sydney, Australia, 4441-4444.